JGR Atmospheres

RESEARCH ARTICLE
10.1029/2024JD042108

Influence of Soil Moisture on the Development of Organized Convective Systems in South America

Laura Paccini[1,2] **and Kathleen A. Schiro**[1]

[1]University of Virginia, Charlottesville, VA, USA, [2]Now at Pacific Northwest National Laboratory, Richland, WA, USA

Key Points:

- The initiation and organization of deep convective systems are encouraged by large soil moisture (SM) gradients
- The relationship between SM heterogeneity and convective system size is evident in simulations both with and without interactive SM
- The impact of SM gradients on convective system size is most pronounced in the absence of large-scale synoptic influences

Supporting Information:

Supporting Information may be found in the online version of this article.

Correspondence to:

L. Paccini,
laura.paccini@pnnl.gov

Citation:

Paccini, L., & Schiro, K. A. (2025). Influence of soil moisture on the development of organized convective systems in South America. *Journal of Geophysical Research: Atmospheres*, *130*, e2024JD042108. https://doi.org/10.1029/2024JD042108

Received 1 AUG 2024
Accepted 20 APR 2025

Author Contributions:

Conceptualization: Laura Paccini, Kathleen A. Schiro
Formal analysis: Laura Paccini
Funding acquisition: Laura Paccini, Kathleen A. Schiro
Methodology: Laura Paccini
Supervision: Kathleen A. Schiro
Visualization: Laura Paccini
Writing – original draft: Laura Paccini
Writing – review & editing: Laura Paccini, Kathleen A. Schiro

Abstract This study investigates the role of soil moisture (SM) on the initiation and organization of convective systems using the convection-permitting ICOsahedral Non-hydrostatic (ICON) model. We conduct two sets of experiments: a Control experiment with interactive SM and a fixed SM experiment (FixedSM) with invariable SM conditions. We focus on two regions in South America: the Amazon and southeastern South America (SESA). Larger organized convective systems are associated with greater SM heterogeneity in both regions, though other large-scale synoptic influences affect the robustness of this relationship in SESA. These results remain largely unaffected by disabling the effects of precipitation on SM in the FixedSM experiment, and complementary analyses using satellite-based estimates of SM and precipitation support these findings. Spatial compositing of mesoscale environments in the Amazon shows the presence of well-defined SM gradients, at a length scale of a few hundred kilometers, many hours ($\mathcal{O}(10)$) before convective system detection. Larger SM gradients correspond to larger gradients in thermodynamic variables, particularly surface temperature and sensible heat flux, and are associated with larger convective systems. Overall, our findings suggest that surface heterogeneities such as SM gradients not only affect deep convection initiation, as previously suggested, but they can also encourage the growth and organization of convective systems into larger clusters, particularly in the absence of significant synoptic influences.

Plain Language Summary Understanding how soil moisture (SM) affects precipitation is crucial for predicting heavy rainstorms. This study explores how variations in SM impact the formation and growth of storms in the Amazon and Southeastern South America (SESA). Using a high-resolution weather model, we find that when there is more spatial variation in SM, larger and more organized storms form. This relationship holds true for both regions, although large-scale weather patterns influence this relationship in SESA. Distinct SM gradients emerge well before storms begin, with stronger gradients leading to larger storms.

1. Introduction

Soil moisture (SM) is a key element of land surface processes and is linked with various processes in the water cycle, ultimately affecting precipitation patterns. Despite its significance, our understanding of SM interactions with organized precipitation, particularly with organized convective systems that often lead to extreme weather events, remains constrained by the uneven distribution and scarcity of observational data in several regions, as well as limitations in numerical forecasting (Liu et al., 2022, and references therein). In this study, we employ convection-permitting simulations to investigate the potential impact of SM on the development of organized convective systems over two distinct regions in South America.

Organized convective systems contribute up to 50% of the total rainfall in the Amazon and up to 60% in southeastern South America (SESA) (Feng et al., 2021), serving as primary drivers of extreme precipitation (Roca & Fiolleau, 2020), which significantly impacts populations and ecosystems. Understanding the dynamics of these systems, however, presents a challenge due to the lack of observations and constraints of conventional models that rely on parameterized convection. These models struggle to accurately represent structured convective entities; they also struggle to represent interactions between SM and precipitation (Taylor et al., 2013), which may be due to sensitivities of land-atmosphere coupling to parameterization choices (Williams, 2019). Therefore, the use of convection-permitting simulations becomes essential for advancements in our understanding of convective systems, as they enable us to reasonably test hypotheses regarding SM controls on convective systems and their evolution.

The coupling between SM and precipitation can be locally understood through modifications in the boundary layer, where SM can affect the partitioning of surface turbulent fluxes. This partitioning affects temperature and

moisture patterns in the boundary layer, which in turn influence convection and precipitation (e.g., Findell & Eltahir, 2003; Pal & Eltahir, 2001) through their effects on instability. Another more indirect way through which SM can impact convection involves mesoscale circulations, where SM gradients induce surface heterogeneity and drive circulations that promote moisture convergence and convective initiation (Pielke, 2001). In this context, Taylor et al. (2012) emphasized the role of mesoscale circulations in triggering convection and favoring afternoon rainfall over dry soils globally. Moreover, Hsu et al. (2017) underscored the role of SM heterogeneity in conditioning the spatial coupling of SM and precipitation, showing a larger preference for precipitation over drier soils under more heterogeneous SM conditions. Other studies, however, emphasize that the mean SM exerts a stronger influence on the overall precipitation response than the spatial pattern of SM (e.g., Baur et al., 2018; Schneider et al., 2019). While these studies address precipitation events, they do not focus on how SM may affect the organization of deep convection.

The influence of SM heterogeneity on deep convection has been largely explored in the context of convective initiation (e.g., Barton et al., 2021; Baur et al., 2018; Chug et al., 2023; Froidevaux et al., 2014; Gaal & Kinter, 2021; Graf et al., 2021; Petrova et al., 2018; Taylor, 2015; Taylor et al., 2011; Teramura et al., 2019). For instance, Taylor et al. (2011) used satellite data to show that SM heterogeneity at spatial scales of 10–40 km promotes low-level convergence, thereby facilitating storm initiation in the Sahel region. Subsequent research demonstrates that the spatial extent of SM heterogeneity effects can extend up to 100 km (e.g., Chug et al., 2023; Gaal & Kinter, 2021; Petrova et al., 2018). Additionally, thermally-induced circulations associated with SM heterogeneity are shown to possibly lead to an earlier onset of deep convection (e.g., Baur et al., 2018; Petrova et al., 2018). While the impact of SM gradient strength may vary by region (Graf et al., 2021; Taylor, 2015), there is consensus that areas with greater SM heterogeneity are more prone to convective initiation.

In contrast, the influence of SM on the upscale growth of larger, organized mesoscale convective systems largely remains to be tested, although a few studies have pointed to the importance of SM heterogeneity at the initial stages of these systems in certain regions (Gaal & Kinter, 2021; Petrova et al., 2018; Taylor, 2015; Teramura et al., 2019). For instance, Klein and Taylor (2020) emphasized the role of SM heterogeneity in favoring the intensification of mature storms at scales of hundreds of kilometers in the Sahel. While these studies are often conducted in semi-arid regions where the influence of SM on deep convection is more direct, the impacts of SM gradients at convective scales under more humid and homogeneous surface conditions, like those in the Amazon, remain considerably less investigated.

Environmental factors further modulate the impact of SM heterogeneity on deep convection. Under conditions of weak synoptic forcing, larger SM gradients enhance the sensitivity of deep convection to SM anomalies (Baur et al., 2018; Chug et al., 2023; Froidevaux et al., 2014; Gaal & Kinter, 2021; Graf et al., 2021; Taylor, 2015). Elevated topography (above 500 m) or complex topographic features can reduce the influence of SM heterogeneities on the precipitation response, as mountain-valley circulations become the predominant atmospheric processes (Barton et al., 2021; Chug et al., 2023). Vegetation cover is also related to SM gradients, with densely vegetated regions typically exhibiting more stable SM conditions given their wetter conditions and deeper rooting systems, while sparsely vegetated areas may show stronger SM gradients conducive to storm initiation (Barton et al., 2021; Chug et al., 2023).

In this study, we aim to characterize the relationship between SM and the development of organized convective systems at sub-daily timescales, as determined by convective system size, precipitation intensity, and duration. We first explore these interactions using a control experiment, where the spatial mean and heterogeneity of SM environments preceding system development are defined as metrics and related to convective growth characteristics. Subsequently, we compare these results with those from a simulation in which SM does not respond to precipitation, helping us to isolate the potential influence of SM characteristics on the growth of an organized convective system. Our modeling framework accounts for a realistic spatial distribution of SM, unlike idealized simulations with imposed SM patterns. We focus on two regions, namely the Amazon and SESA, which are characterized by distinct SM regimes. The Amazon represents a tropical rainforest, characterized by more homogeneous and generally wetter SM conditions, with a weaker synoptic influence compared to SESA, a subtropical transition zone with both dry and wet climates. Studying the Amazon offers an opportunity to explore the potential role of SM in controlling deep convective growth in the absence of strong synoptic forces, while SESA provides insights into these relationships in a region with expected direct soil-atmosphere interactions. Given the ongoing changes in land cover, including deforestation, and their implications for both regional and global

climate patterns (Werth & Avissar, 2002), elucidating these interactions is essential and has direct relevance for predicting and managing the effects of climate variability and climate change.

2. Model and Experimental Setup

We use the ICOsaedral Non-hydrostatic (ICON) atmospheric model (Zängl et al., 2015) in its numerical weather prediction (NWP) configuration, version 2.6.4. Physical parameterizations common to all domains include the Rapid Radiative Transfer Model (RRTM; Mlawer et al., 1997) for the radiation scheme, the single-moment microphysics scheme (Doms et al., 2021) and the turbulent kinetic energy scheme (Raschendorfer, 2001). The bulk mass-flux convective parameterization (Bechtold, 2017) is only active for the global simulation.

The ICON-NWP model uses the interactive multi-layer land scheme TERRA_ML (Doms et al., 2021) to parameterize land surface processes. Soil water content is predicted based on the Richardson equation across eight soil layers, extending to a depth of 14.58 m. The TERRA_ML scheme accounts for evapotranspiration, infiltration, percolation, capillary movement, runoff, as well as melting and freezing of snow. Vegetation is prescribed by monthly varying leaf area index, fractional plant cover and root depth. To address subgrid surface variability, three dominant surface types within each grid cell are dynamically chosen to be represented by tiles, based on their fractional area coverage. Additional tiles, representing water bodies like open water, lake, and sea-ice, may be included when significant.

Surface fluxes of heat and moisture are parameterized using a drag-law formulation, requiring potential temperature and humidity inputs from both the first atmospheric level and the land model. The latent heat flux (LHF) (evaporation), computed by TERRA-ML at the grid box level, comprises contributions from bare soil evaporation (Schulz & Vogel, 2020), sublimation from snow, evaporation from the interception store, and plant transpiration, weighted by their respective area. Interception evaporation depends on potential evaporation metrics and the total content of the interception reservoir. Transpiration only occurs when surface conditions direct evaporation to the atmosphere, following Dickinson (1984); otherwise, it is suppressed.

Initial conditions for the atmosphere, SM, soil, and surface temperatures, are derived from the European Centre for Medium-Range Weather Forecasts (ECMWF) and Integrated Forecast System (IFS) operational analysis. Grids and external parameters (e.g., land properties such as soil type, vegetation characteristics, orography, etc.) are retrieved from the Online Grid Generator tool from the German Meteorological Service (DWD; Web Services of Deutscher Wetterdienst, 2021). This web interface uses the ICON tools version 2.5.1 (Prill, 2020) and software tool External Parameter for Numerical Weather Prediction and Climate Application (EXTPAR; Asensio et al., 2020) which provides grids and external parameters, respectively.

We conduct two sets of simulations utilizing a global simulation framework with regional refined mesh capabilities. The global simulation operates at a grid spacing of 20 km and provides initial and boundary conditions to one-way nested domains at 10 and 5 km (Figure S1 in Supporting Information S1). We only analyze the innermost domain, which bounds the region 83°W–33°W; 30°S–20°N. In all domains the vertical resolution includes 90 levels, with the model top at 75 km.

The first set of simulations serves as our Control experiment, running for a total of 50 days. We analyze only the final 20 days to allow SM conditions to stabilize, a decision driven by the high computational costs and supported by visual inspections showing that the most significant decreases in SM occurred during the initial 30-day period (Figure S2 in Supporting Information S1). The second set of simulations, named the FixedSM experiment, restarts on day 31 from the Control experiment and runs for 20 days. In this setup, SM values remain constant based on the initial conditions from the restart date. Given the minimal diurnal (<1 kg m^{-2}) and intraseasonal (<5 kg m^{-2}) variability relative to the domain-mean values (on the order of 100 kg m^{-2}), we find this approach justified for the scope of our relatively short-duration study (Figure S2 in Supporting Information S1). This configuration allows us to study how variations in SM conditions affect convective system properties. Although SM conditions are fixed, variability in LHF can occur through canopy interception, an important process in tropical areas. A discussion on the differences between the Control and FixedSM experiments regarding SM-atmosphere interactions will be provided in Section 5.

Three ensemble members are conducted for each set of simulations to account for atmospheric variability within computational constraints, given the high resolution (5 km) of the 50-day simulations. Each of these members starts on different days in early March 2017, a period selected for high organized convection frequency (Rehbein

et al., 2018). Although the choice of the year was arbitrary, 2017 being an ENSO-neutral year helps reduce potential confounding effects from ENSO phases. Simulations are initialized using IFS analysis and assimilate SST data every 15 days, allowing the atmospheric conditions to freely evolve.

3. Data and Methods

3.1. Data

To compare our simulations with observations, we use satellite-based estimations from the Integrated Multi-satellite Retrievals (IMERG) precipitation data set V6 (Huffman et al., 2019) and the Level 4 product from the Soil Moisture Active Passive (SMAP-L4 Version 7; Reichle et al., 2022) data set. The IMERG product features a grid spacing of approximately 10 km and provides data updates every 30 min. The SMAP L4 product integrates SMAP brightness temperature observations into a land surface model, employing a grid spacing of 9 km to generate 3-hourly outputs. SM from this product is quantified as the water content within a depth of 1 m.

Given the overall dense canopy in the Amazon, the microwave signals from the SMAP satellite are attenuated, making it difficult for the satellite to detect the SM beneath. As a result, direct SMAP observations have reduced reliability in these areas (e.g., Dong et al., 2019), and the SM estimates in the SMAP L4 product over the Amazon are primarily driven by the land surface model. Despite these uncertainties, supplementary analysis (not shown) indicates that the SMAP-L4 product captures distinct SM patterns related to the size of convective systems, consistent with our simulation results, thereby supporting its use in our analysis.

3.2. Definition of Convective Systems

As a first step, following Paccini and Stevens (2023), we initially define hourly precipitating objects as those 8-way contiguous grids (west–east, north–south, northeast–southwest, northwest–southeast) where precipitation exceeds 1 mm hr^{-1} per grid cell and whose total area is at least 2,500 km^2. These criteria are adjusted from Paccini and Stevens (2023) to enhance the detection of the initial stages of convective systems. Next, we apply the tracking algorithm from the Tracking and Object-Based Analysis of Clouds TOBAC v1.4.2, which predicts the location of the precipitating object in the next timestep using its average propagation speed from the previous timesteps (Heikenfeld et al., 2019). Only those convective systems that persist for more than 3 hr are retained for further analysis.

In our study, we employed the TOBAC algorithm, which has demonstrated robust results using various thresholds to define precipitating systems. While differences in mesoscale convective system statistics can arise from variations in tracking algorithms, as discussed by Prein et al. (2024), our analysis prioritizes consistency within the chosen framework. The potential influence of different tracking algorithms on results is acknowledged, though not exhaustively explored in this study.

To systematically examine the lifecycle of identified convective systems, we classify each one into distinct stages, where a "stage" represents a temporal segment whose length varies according to the system's total lifespan. Systems lasting fewer than 7 hr are given two initial and two final stages, with the remaining timesteps classified as intermediate. For longer-lived systems, the first three and last three timesteps are marked as initial and final stages, respectively, with the rest labeled as intermediate.

To define the convective systems in observations, we implement the detection and tracking algorithms on the hourly-accumulated IMERG precipitation data. After the systems are identified and their tracks established, we sub-sample the data of these tracked systems to align with the 3-hourly intervals of the SMAP SM outputs. This sub-sampling process retains only the timestamps of systems that coincide with the SMAP observation times for subsequent analysis.

Our analysis focuses on the Amazon and SESA regions, defined as 15 × 10° boxes. Only systems that have at least the initial and intermediate stages occurring within these analysis regions (outlined in red boxes in Figure S1 in Supporting Information S1) are selected for further analysis. This approach ensures our focus remains on developing systems.

3.3. Definition of Environmental SM

To associate features of convective systems with the state of SM in the nearby environment, we define the environment as the area delimited by two times the equivalent radius of each system from its center of mass in both horizontal and meridional directions. The center of mass for each convective system is determined by calculating the weighted centroid, which is based on the spatial distribution of precipitation within the system. Sensitivity tests considering larger areas up to four times the equivalent radius of the system lead to similar results. Similarly, our results are robust to defining the environment using a constant area (Figure S3 in Supporting Information S1), as there is no clear relationship between area and heterogeneity (Figure S4 in Supporting Information S1).

To characterize the environmental SM, we compute the spatial mean and heterogeneity of SM on the original output (5 km) after omitting grid cells with rivers (land fraction <1) and high topography (>500 m) to avoid drastic gradients. The mean value considers the water soil content within the first five layers (0.54 m). Heterogeneity of SM is measured as the spatial standard deviation of SM in the defined environment. To ensure the robustness of our SM-heterogeneity definition, supplementary metrics of SM heterogeneity were introduced, capturing broader spatial patterns influencing convective systems (not shown). These calculations are performed 6 hr before system detection to ensure that we assess pre-storm environmental conditions, complementing the FixedSM setup.

4. Sensitivity of Convective System Features to SM Metrics

In what follows, we characterize the pre-convective environment 6 hr before the detection of growth-phase organized convective systems in both the Amazon and SESA and investigate relationships between SM conditions and convective system characteristics (precipitation intensity, convective system size and duration). Though we are careful to sample the pre-convective environment, we perform an additional analysis to remove any effects of the convective system on the soils through precipitation by fixing SM content to determine whether any emergent SM-convection relationships are dependent on these interactions (FixedSM experiment).

Convective systems are identified and tracked using the TOBAC tracking algorithm (see Section 3.2). During the study period, the Amazon region exhibited significantly higher convective activity compared to SESA, with approximately 200 convective systems identified in the Amazon and about 50 in SESA. The median lifetime of these systems is 5 hr, with the 90th percentile reaching around 8 hr, showing consistency across both regions.

To investigate how SM conditions relate to convective system characteristics, we define two regimes in the SM metrics within the nearby environment 6 hr prior to convective system detection. The definitions of the environment and SM metrics are detailed in Section 3.3. High regimes for SM mean or SM heterogeneity are defined as values within the 50th to 90th percentiles, while low regimes include values within the 10th to 50th percentiles. This range selection avoids extreme values and focuses our analysis on representative patterns. We evaluate these relationships within each experiment and in observations to assess robustness.

Figures 1 and 2 illustrate the percentage changes in the size, intensity and duration of convective systems when considering high and low regimes of SM mean and SM heterogeneity for the Amazon and SESA regions, respectively. A positive value indicates an increase in the given feature for the high regime relative to the low regime. Overall, significant changes are more pronounced when considering SM heterogeneity than when considering SM mean. In particular, convective system size exhibits the most robust response across data sets and between the two regions, increasing as SM heterogeneity increases.

In the Control simulation, significant relationships are observed between SM heterogeneity and convective system size, mean and maximum precipitation, and duration in the Amazon. In SESA, these relationships are only significant for size and maximum precipitation. The mean size of convective systems increases by 43.2% in the Amazon region (57% in SESA) when the environment is characterized by high SM heterogeneity compared to low SM heterogeneity (Figures 1 and 2). Systems developing over high SM heterogeneity environments last roughly 5% longer in the Amazon, though these changes are negligible in SESA. Moreover, while mean and maximum precipitation reduce in high SM heterogeneity environments in the Amazon, they increase in SESA. Finally, high SM mean conditions relate to larger convective systems in the Amazon, but no significant relationships between convective system characteristics and SM mean are found in SESA.

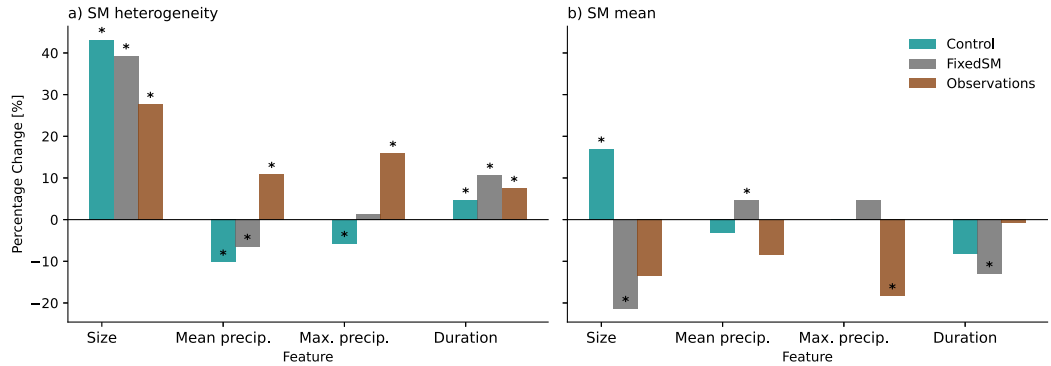

Figure 1. Percentage change in convective system features between high and low regimes of (a) soil moisture (SM) heterogeneity and (b) SM mean, based on SM conditions 6 hr prior to system detection in the Amazon region. An asterisk indicates statistically significant differences determined by the Mann-Whitney test (p-value <0.05).

To discern which SM influences are robust to the potential impact of precipitation, we examine these relationships in the FixedSM experiment. In both the Amazon and SESA, the relationship between convective system size and SM heterogeneity remains pronounced, suggesting that an enhancement in SM heterogeneity from the precipitation resulting from the convective systems is not driving this relationship. For the Amazon, the relationships between SM heterogeneity, mean precipitation, and system duration appear to be robust to any confounding influence of precipitation on SM. Interestingly, the relationship between SM mean and convective system size reverses in the FixedSM experiment for the Amazon, where a decrease in mean SM increases the convective system size. This discrepancy suggests that SM mean may not be a robust metric for assessing convective system characteristics. While additional statistically significant relationships emerge within the FixedSM experiment (e.g., an increase in precipitation related to an increase in mean SM), our focus remains on relationships consistent across both experiments.

As an additional test of robustness, we compare our results to observations using SMAP SM and IMERG precipitation (Section 3.1). In summary, the most robust relationship comparing SM characteristics to convective system characteristics is between SM heterogeneity and convective system size, which is of the same sign and statistically significant in both model experiments; it is also statistically significant in the Amazon in observations but not in SESA. While SMAP observations provide valuable insights due to their calibration with IMERG precipitation, offering good correspondence between SM and precipitation, it is important to note that the SMAP satellite measures SM once per day. This infrequent observation can present challenges in confirming that SM is unaffected by precipitation at specific times. Additionally, accurately retrieving SM beneath dense tropical forests remains challenging for SMAP, adding uncertainty to its estimates in this region. Furthermore, SMAP measures SM to a depth of about 1 m, differing from the 0.54 m considered in our simulations. These factors should be considered when interpreting the observational data.

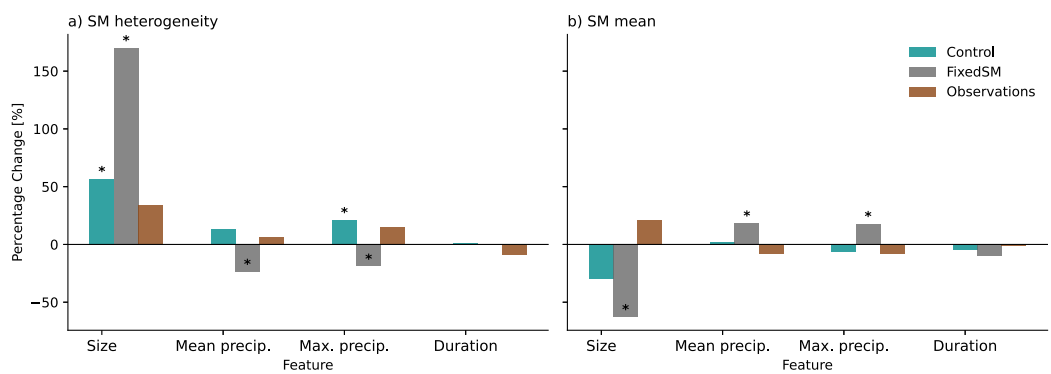

Figure 2. As in Figure 1, but for the southeastern South America region.

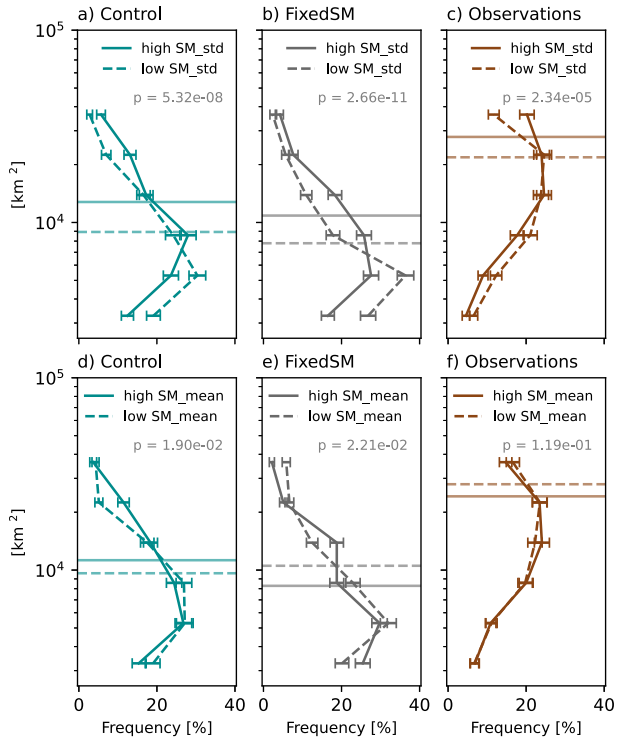

Figure 3. (a–c) Size distribution of convective systems by regime of soil moisture (SM) heterogeneity and (d–f) SM mean 6 hr before the system detection, for simulations and observations in the Amazon region. Regimes of high SM heterogeneity or mean (solid lines) represent values between the 50th and 90th percentiles of their respective metrics, while regimes of low SM heterogeneity (dashed lines), represent values between the 10th and 50th percentiles. The *p*-values for differences between regimes, calculated using the Mann-Whitney test, are also indicated. Solid and dashed horizontal lines indicate the mean values of the high and low SM regime, respectively.

A closer examination of how these SM metrics relate to convective system size is provided in Figures 3 and 4. These figures demonstrate that the size distribution shifts toward bigger systems in high SM heterogeneity regimes compared to low SM regimes. Conversely, variations in SM mean yield inconsistent results across regions and data sets (as shown in Figures 1 and 2). They also illustrate that changes in convective system features tend to be more robust in the Amazon. This difference in robustness may relate to the greater number of cases analyzed in the Amazon in comparison to SESA. It is also important to note that a greater number of additional factors could influence convective systems in SESA. Contributing factors include large-scale conditions such as significantly lower associated column water vapor in SESA compared to the Amazon (Figure S5a in Supporting Information S1). Additionally, stronger surface winds in SESA (Figure S5b in Supporting Information S1) could be indicative of greater wind shear, possibly contributing to the organization of convection into larger, more intense systems. This complexity makes isolating the specific impact of SM heterogeneity challenging without controlling for these factors in SESA. In contrast, the Amazon's more uniform conditions offer a clearer perspective on how SM heterogeneity impacts convective system size. Consequently, the following analysis will focus exclusively on the Amazon region and the relationships between near-surface thermodynamic and dynamic conditions, SM heterogeneity, and convective system size.

5. Environmental Conditions Related to SM Heterogeneity

Next, we examine the spatial composites of environmental variables and their relationship to SM heterogeneity and convective system size. Our expectation is that spatially compositing SM anomalies for big and small systems separately will reveal larger SM gradients for big systems than small systems. Spatial composites of environmental variables will then provide insights into how SM influences boundary layer conditions, potentially fostering convective system initiation and organization.

To build composites of big and small systems, we consider the cases within the 50th–90th percentile of the size distribution as big systems, and those within the 10th–50th percentile as small systems, based on their sizes at the initial stage of the convective lifecycle. Note that the initial stage size (see Section 3.2 for definition) correlates strongly with both the mean ($R = 0.92$) and maximum size ($R = 0.86$) throughout the system's lifecycle. For the Control experiment, the size range of big systems is approximately 6,000 km^2 to 15,000 km^2 and for small systems, it is 3,000 km^2–6,000 km^2. In the FixedSM experiment, these ranges are 5,000 km^2 to 16,000 km^2 for big systems and 3,000 km^2–5,000 km^2 for small systems. The composites consider cases that propagate with direction angles between −135° and 135°, capturing the predominant westward propagation which includes movement from the northwest through west to southwest.

By compositing the SM based on the size (big or small) of convective systems (Figures 5 and 6), it becomes apparent that larger SM gradients (i.e., more spatially heterogeneous) are related to bigger systems (bottom rows in Figures 5 and 6). These SM gradients, depicted at a length scale of about 220 km, are found up to 24 hr before a convective system develops. High contrasts of SM in the near environment where convection develops appear to amplify gradients of humidity and temperature at the surface, which become further enhanced 6 hr prior to convection development through enhanced surface convergence along the dry/warm and moist/cool boundaries. Additionally, while the mean surface winds are predominantly westward, their spatial anomalies show an outflow boundary at the surface ahead of the convective system at Time = 0 hr, which converges moisture. This effect may be further enhanced by moister soils. These findings suggest that areas with drier soils and enhanced surface convergence along dry-moist boundaries support convective initiation, while convective systems mature as they propagate over moister soils.

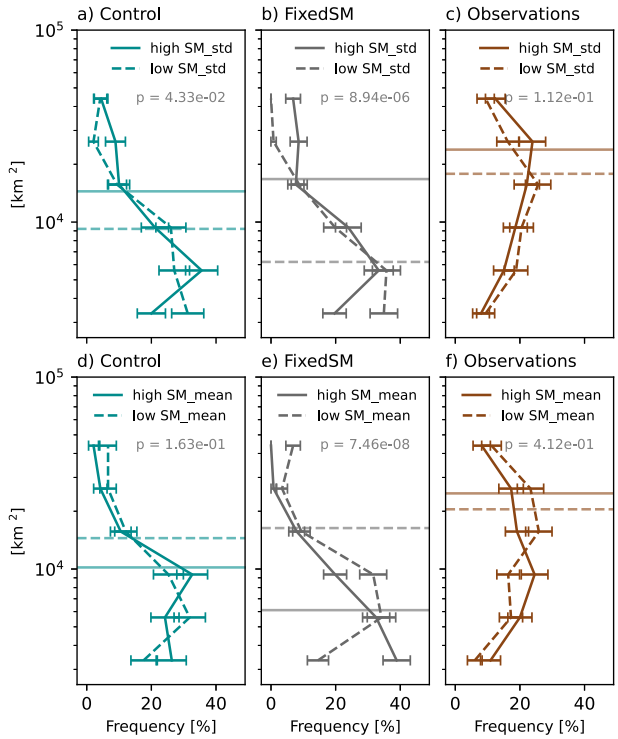

Figure 4. As in Figure 3, but for southeastern South America.

Similar environmental conditions are observed for both the Control and FixedSM experiments: big convective systems develop over areas with stronger SM gradients than small systems, which reflect in larger moisture and temperature perturbations. Although SM patterns structurally differ in the FixedSM experiment (Figure 6), strong and weak gradients in surface temperature and humidity for big and small systems remain consistent up to 24 hr before system detection.

To further explore how SM conditions influence the boundary layer via surface fluxes, Figures 7 and 8 present the composite evolution of the Evaporative Fraction (EF, the ratio of latent to sensible plus latent heat), mean SM, LHF, sensible heat flux (SHF), and to assess the potential influence of pre-convective cloud cover, we also include the shortwave cloud radiative effect (SWCRE, the difference between clear-sky shortwave radiation and the actual shortwave radiation at the surface) for all westward-propagating systems in the Control (Figure 7) and FixedSM (Figure 8) experiments, depicted from 6 hr before detection. We specifically examine these quantities during the morning hours leading up to the detection of convective systems, targeting key periods within the diurnal cycle when SM has the most impact on surface evaporation rates and boundary layer processes, potentially affecting subsequent storm organization.

The composite fields reveal mixed influences from SM and SWCRE on surface fluxes. Regions with higher SWCRE experience reduced net shortwave radiation, which corresponds to regions of reduced EF, LHF, and SHF, indicating that SWCRE modulates the energy available for surface fluxes. Despite this added complexity introduced by cloud cover, a consistent link remains between SM and SHF, with high values of SHF in the northeastern domain aligning with lower SM values in both experiments.

A spatial correlation analysis indicates that pre-convective cloud cover provides the dominant control on the observed variations in surface fluxes (Figure S6 in Supporting Information S1), yet a significant relationship persists between SM, SHF and surface temperature. In contrast, the correlation between SM patterns and LHF is less robust (strong correlations in the FixedSM experiment and weak in the Control experiment; Figure S6 in Supporting Information S1). Hence, SM heterogeneity appears to influence convective system size primarily through its modulation of SHF, which fosters convective instability and anomalous circulations that promote the growth of developing convection along pronounced SM gradients. Additionally, enhanced surface convergence along the dry-moist boundary (see Figures 5 and 6) would support convection.

In summary, the interplay among SM heterogeneity, cloud cover, and surface fluxes adds complexity to land-atmosphere interactions in this region. Nonetheless, the consistent relationship between SM heterogeneity and convective system size suggests that SM patterns are an important contributing factor in convective organization, primarily through their influence of sensible heat fluxes and subsequent boundary-layer dynamics, in the absence of strong synoptic influences.

6. Summary and Conclusions

In this study, we investigate the impact of SM on organized deep convection in the Amazon and SESA. We use a convection-permitting model with a 5 km grid spacing and incorporate satellite-based products of precipitation and SM.

We first explore which mesoscale characteristics of organized convective systems appear to be most affected by SM, using ensemble simulations with the ICON-NWP model coupled to a multi-layer land scheme, which enables SM–atmosphere interactions. This ensemble is referred to as the Control experiment. We relate convective system size, intensity, and duration to SM heterogeneity and mean, defined 6-hr prior to the system initiation. Our most robust conclusion is a relationship between convective system size and SM heterogeneity, with larger ("more organized") systems occurring in regions with larger SM gradients. In SESA, while convective system size

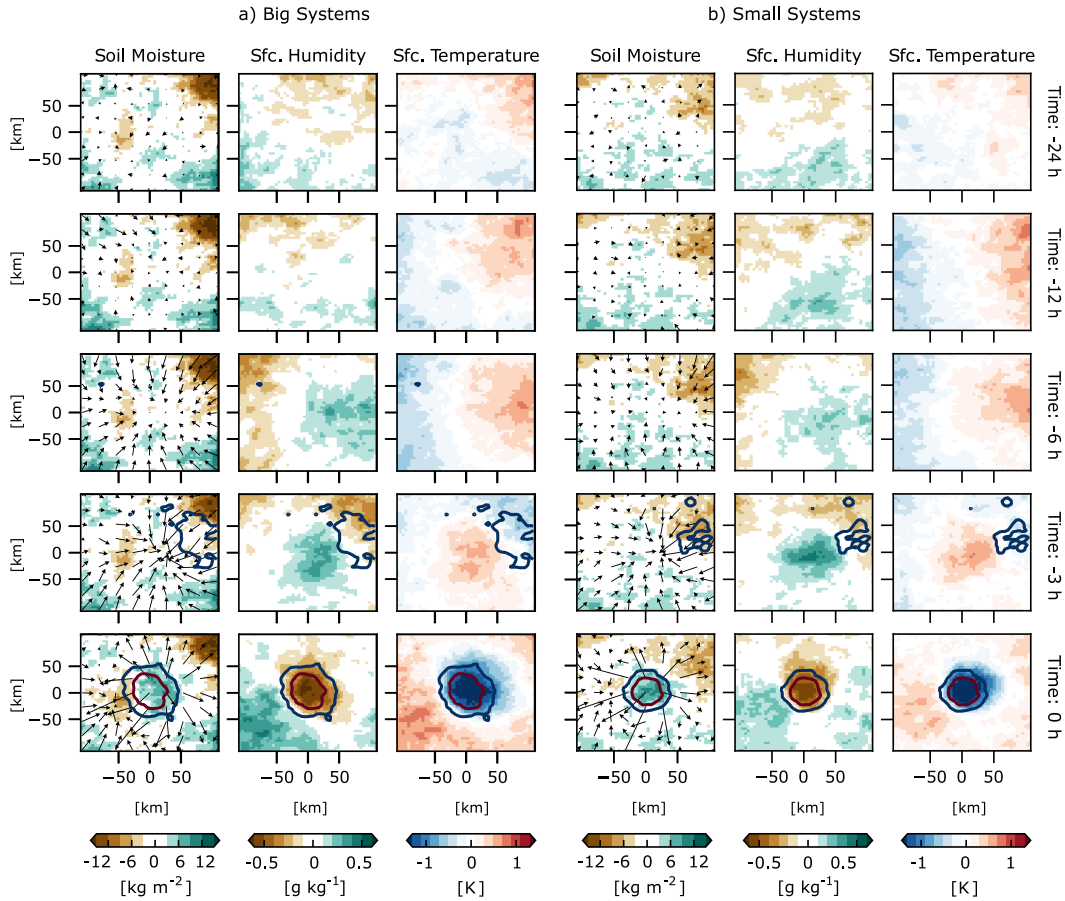

Figure 5. Composite evolution of convective system growth for (a) big and (b) small systems in the Control experiment that propagate westward in the Amazon. Columns show soil moisture, surface humidity, surface temperature (shaded), precipitation (contours) and 10-m winds (vectors). The analysis spans 24, 12, 6, and 3 hr before system detection. The bottom row in both panels displays the instance of convective system detection, centered at (0,0). The size classification is based on percentiles (50th to 90th for big systems and 10th to 50th percentile for small systems). Anomalies are calculated with respect to the spatial mean. Contours represent 1 and 5 mm hr^{-1} precipitation anomalies.

generally increases with SM heterogeneity, the results are less robust and potentially influenced by additional factors, including lower mean column moisture and stronger winds (increased wind shear). A secondary set of simulations where SM features remain unaffected by atmospheric feedbacks by keeping SM constant over time (FixedSM experiment) is then analyzed and compared to the Control simulations to more directly isolate emergent SM-convection relationships. The consistency of the relationship between SM heterogeneity and system size across both experiments suggests that SM heterogeneity enhances system size, rather than the system size altering SM heterogeneity through precipitation.

To further investigate the role of SM heterogeneity on convective system organization in the Amazon, we perform a composite analysis comparing thermodynamic environments of big and small convective systems. Our spatial composite analysis reveals that SM heterogeneity is detected well before system development, identified up to 24 hr in advance. Larger SM gradients in the mesoscale convective environment, shown at a length scale of a few hundred kilometers, are associated with larger systems. These SM gradients imprint upon the surface humidity, air temperature, and surface fluxes, in particular the surface temperature and SHF. Additionally, our analysis shows that cloud cover, through the SWCRE, also modulates surface fluxes and adds complexity to these interactions. Despite the influence of cloud cover, these results suggest that convection initiates over drier soils and matures over wetter soils, which is consistent with findings from semi-arid regions (e.g., Chug et al., 2023; Klein & Taylor, 2020; Taylor et al., 2011).

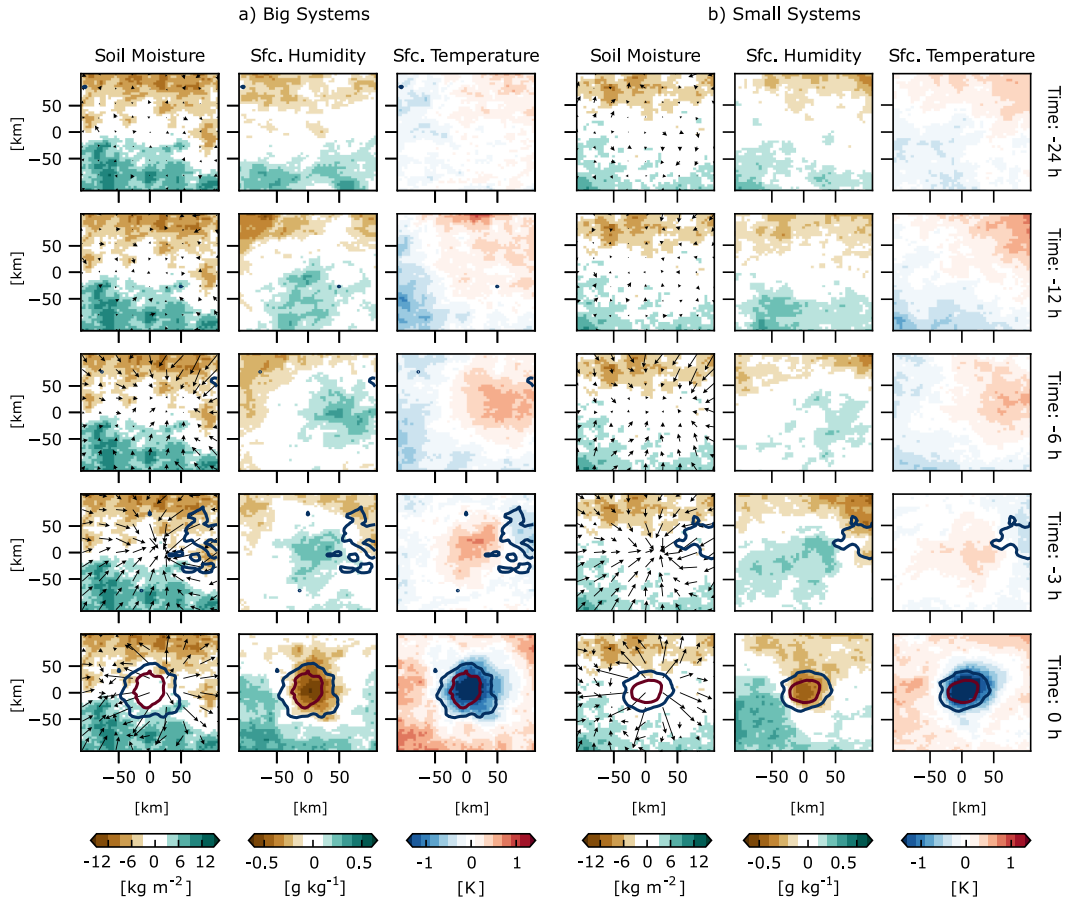

Figure 6. Composite evolution of convective system growth for (a) big and (b) small systems in the FixedSM experiment as in Figure 5.

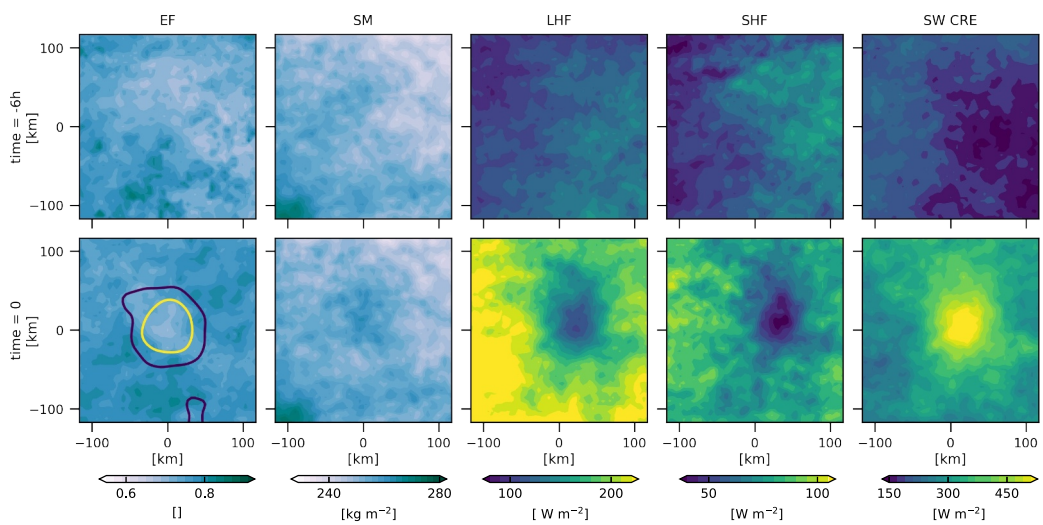

Figure 7. Composite evolution of evaporative fraction, mean soil moisture, latent heat flux, sensible heat flux, and shortwave cloud radiative effect for all westward-propagating systems in the Control experiment from 6 hr before detection. Only systems first identified between 12 and 18 hr are shown for time = 0. Contours represent 2 and 5 mm hr^{-1} precipitation values.

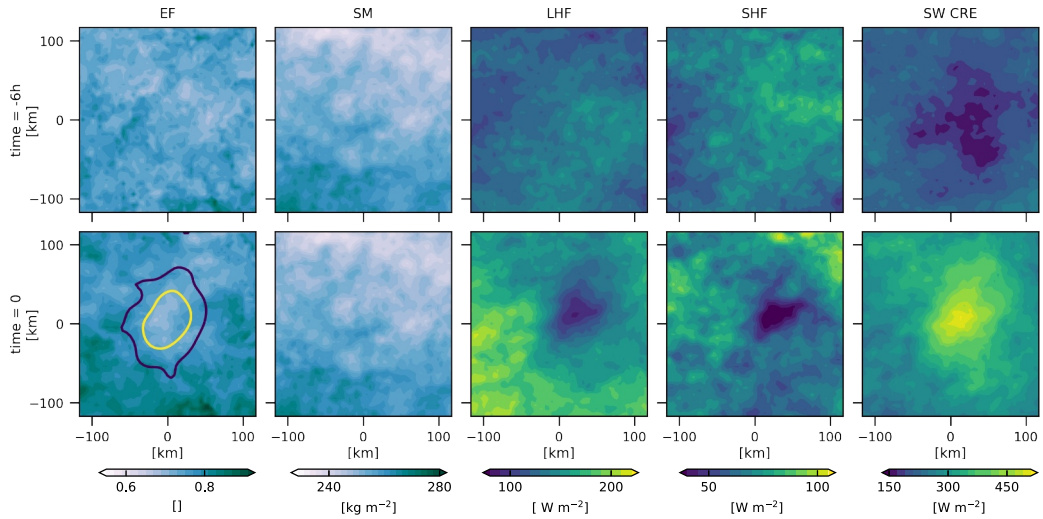

Figure 8. Composite evolution of evaporative fraction, mean soil moisture, latent heat flux, sensible heat flux, and shortwave cloud radiative effect in the FixedSM experiment as in Figure 7.

In summary, our results suggest that SM heterogeneity plays an important role in conditioning boundary layer thermodynamics to favor convective system growth and organization. The consistent findings across both FixedSM and Control experiments, as well as in observations, suggest robustness of this relationship. While fully isolating the effects of SM requires further investigation, spatial and temporal analyses indicate that enhanced surface convergence along moist-dry soil boundaries, modulated by both SM and SWCRE, creates a favorable environment for the initiation and subsequent growth of convective systems.

However, some important caveats should be noted. As discussed previously, limited direct SM observations in this region make it difficult to characterize SM variability and verify our results. The scarcity of atmospheric thermodynamic and surface flux measurements further complicates observational analyses linking SM to atmospheric processes. Moreover, our model simulations may contain biases in their representation of SM-convection interactions, potentially overemphasizing SM gradients that may be weaker or absent in densely forested regions in reality. Nevertheless, we argue that our simulations offer valuable insights into the general relationships among SM, surface thermodynamics, and storm organization. Additionally, while our focus here is specifically on SM, we conjecture that other surface heterogeneities modifying surface fluxes similarly might also influence the organization of deep convection.

Future work should extend this investigation to other regions, especially where dense observational networks would permit a more comprehensive observational analysis of SM-convection coupling. It would also be beneficial to explore how different types of surface heterogeneity, such as changes in land use and land cover (LULCC), affect deep convection organization, as LULCC is known to induce mesoscale circulations (Wang et al., 2009). For instance, previous studies have found conflicting results regarding Amazon deforestation impacts, with some indicating reductions in overall precipitation (e.g., Silva et al., 2016; Werth & Avissar, 2002), and others suggesting increased precipitation over deforested areas (e.g., Chagnon & Bras, 2005; Khanna et al., 2017). Improving our understanding of the physical response of convective systems to LULCC may help to answer these important questions.

Data Availability Statement

IMERG data were provided by the NASA Goddard Space Flight Center's IMERG and PPS teams, and archived at the NASA GES DISC (https://disc.gsfc.nasa.gov/datasets/GPM_3IMERGHHL_06/). SMAP-L4 data were provided by the National Snow and Ice Data Center (NSIDC) via HTTPS File System at https://nsidc.org/data/spl4smau/versions/7. Boundaries of the Amazon are available at (Lehner et al., 2006) and were obtained from https://www.hydrosheds.org/products/hydrobasins. The code to make the plots in this paper and to perform the relevant analyses (Paccini, 2024) is available on Zenodo.

Acknowledgments
The authors acknowledge the University of Virginia and the NSF (Award AGS-2225954) for their support of this work. This work is also supported by the Office of Science, U.S. Department of Energy Biological and Environmental Research as part of the Regional and Global Model Analysis program area through the Water Cycle and Climate Extremes Modeling (WACCEM) scientific focus area. PNNL is operated for DOE by Battelle Memorial Institute under contract no. DE-AC05-76RL01830. The authors thank the Max Planck Institute for Meteorology and the German Climate Computing Center (DKRZ) for providing the computer resources necessary to conduct the simulations. The authors thank Drs. Cornelia Klein, Francina Dominguez, and Divyansh Chug for their constructive discussions and comments, as well as the helpful comments from three anonymous reviewers, which substantially improved the manuscript.

References

Asensio, H., Messmer, M., Lüthi, D., & Osterried, K. (2020). External parameters for numerical weather prediction and climate application EXTPAR v5_0. User and implementation guide. Retrieved from http://www.cosmo-model.org/content/support/software/ethz/EXTPAR_user_and_implementation_manual_202003.pdf

Barton, E., Taylor, C., Klein, C., Harris, P., & Meng, X. (2021). Observed soil moisture impact on strong convection over mountainous Tibetan Plateau. *Journal of Hydrometeorology*, *22*(3), 561–572.

Baur, F., Keil, C., & Craig, G. C. (2018). Soil moisture–precipitation coupling over central Europe: Interactions between surface anomalies at different scales and the dynamical implication. *Quarterly Journal of the Royal Meteorological Society*, *144*(717), 2863–2875.

Bechtold, P. (2017). Atmospheric moist convection. *Meteorological Training Course Lecture Series*, 1–78. Retrieved from https://www.ecmwf.int/node/16953

Chagnon, F., & Bras, R. (2005). Contemporary climate change in the Amazon. *Geophysical Research Letters*, *32*(13), L13703. https://doi.org/10.1029/2005GL022722

Chug, D., Dominguez, F., Taylor, C. M., Klein, C., & Nesbitt, S. W. (2023). Dry-to-wet soil gradients enhance convection and rainfall over subtropical South America. *arXiv preprint arXiv:2304.04630*.

Dickinson, R. E. (1984). Modeling evapotranspiration for three-dimensional global climate models. *Climate processes and climate sensitivity*, *29*, 58–72.

Doms, G., Förstner, J., Heise, E., Herzog, H., Mironov, D., Raschendorfer, M., et al. (2021). A description of the nonhydrostatic regional COSMO model. Part II: Physical parameterizations. *Deutscher Wetterdienst, Offenbach, Germany*. https://doi.org/10.5676/DWD_pub/nwv/cosmo-doc_6.00_II

Dong, J., Crow, W., Reichle, R., Liu, Q., Lei, F., & Cosh, M. H. (2019). A global assessment of added value in the SMAP Level 4 soil moisture product relative to its baseline land surface model. *Geophysical Research Letters*, *46*(12), 6604–6613. https://doi.org/10.1029/2019GL083398

Feng, Z., Leung, L. R., Liu, N., Wang, J., Houze Jr, R. A., Li, J., et al. (2021). A global high-resolution mesoscale convective system database using satellite-derived cloud tops, surface precipitation, and tracking. *Journal of Geophysical Research: Atmospheres*, *126*(8), e2020JD034202. https://doi.org/10.1029/2020JD034202

Findell, K. L., & Eltahir, E. A. (2003). Atmospheric controls on soil moisture–boundary layer interactions. Part II: Feedbacks within the continental United States. *Journal of Hydrometeorology*, *4*(3), 570–583.

Froidevaux, P., Schlemmer, L., Schmidli, J., Langhans, W., & Schär, C. (2014). Influence of the background wind on the local soil moisture–precipitation feedback. *Journal of the Atmospheric Sciences*, *71*(2), 782–799.

Gaal, R., & Kinter III, J. L. (2021). Soil moisture influence on the incidence of summer mesoscale convective systems in the US Great Plains. *Monthly Weather Review*, *149*(12), 3981–3994.

Graf, M., Arnault, J., Fersch, B., & Kunstmann, H. (2021). Is the soil moisture precipitation feedback enhanced by heterogeneity and dry soils? A comparative study. *Hydrological Processes*, *35*(9), e14332.

Heikenfeld, M., Marinescu, P. J., Christensen, M., Watson-Parris, D., Senf, F., van den Heever, S. C., & Stier, P. (2019). Tobac 1.2: Towards a flexible framework for tracking and analysis of clouds in diverse datasets. *Geoscientific Model Development*, *12*(11), 4551–4570.

Hsu, H., Lo, M.-H., Guillod, B. P., Miralles, D. G., & Kumar, S. (2017). Relation between precipitation location and antecedent/subsequent soil moisture spatial patterns. *Journal of Geophysical Research: Atmospheres*, *122*(12), 6319–6328. https://doi.org/10.1002/2016JD026042

Huffman, G., Stocker, E., Bolvin, D., Nelkin, E., & Tan, J. (2019). GPM IMERG final precipitation L3 half hourly 0.1 degree × 0.1 degree v06 [Dataset]. *Goddard Earth Sciences Data and Information Services Center (GES DISC)*. https://doi.org/10.5067/GPM/IMERG/3B-HH/06

Khanna, J., Medvigy, D., Fueglistaler, S., & Walko, R. (2017). Regional dry-season climate changes due to three decades of Amazonian deforestation. *Nature Climate Change*, *7*(3), 200–204.

Klein, C., & Taylor, C. M. (2020). Dry soils can intensify mesoscale convective systems. *Proceedings of the National Academy of Sciences*, *117*(35), 21132–21137.

Lehner, B., Verdin, K., & Jarvis, A. (2006). Hydrological data and maps based on SHuttle Elevation Derivatives at multiple Scales (HydroSHEDS)—Technical documentation [Dataset]. *World Wildlife Fund US*. Retrieved from https://www.hydrosheds.org/products/hydrobasins

Liu, W., Zhang, Q., Li, C., Xu, L., & Xiao, W. (2022). The influence of soil moisture on convective activity: A review. *Theoretical and Applied Climatology*, *149*(1–2), 221–232.

Mlawer, E. J., Taubman, S. J., Brown, P. D., Iacono, M. J., & Clough, S. A. (1997). Radiative transfer for inhomogeneous atmospheres: RRTM, a validated correlated-k model for the longwave. *Journal of Geophysical Research*, *102*(D14), 16663–16682. https://doi.org/10.1029/97JD00237

Paccini, L. (2024). Analysis code for Paccini and Schiro 2024—JGRA (version v1) [Dataset]. *Zenodo*. https://doi.org/10.5281/ZENODO.14450911

Paccini, L., & Stevens, B. (2023). Assessing precipitation over the Amazon basin as simulated by a storm-resolving model. *Journal of Geophysical Research: Atmospheres*, *128*(4), e2022JD037436. https://doi.org/10.1029/2022JD037436

Pal, J. S., & Eltahir, E. A. (2001). Pathways relating soil moisture conditions to future summer rainfall within a model of the land–atmosphere system. *Journal of Climate*, *14*(6), 1227–1242.

Petrova, I. Y., Miralles, D. G., Van Heerwaarden, C. C., & Wouters, H. (2018). Relation between convective rainfall properties and antecedent soil moisture heterogeneity conditions in North Africa. *Remote Sensing*, *10*(6), 969.

Pielke, R. A. (2001). Influence of the spatial distribution of vegetation and soils on the prediction of cumulus convective rainfall. *Reviews of Geophysics*, *39*(2), 151–177. https://doi.org/10.1029/1999RG000072

Prein, A. F., Feng, Z., Fiolleau, T., Moon, Z. L., Núñez Ocasio, K. M., Kukulies, J., et al. (2024). Km-scale simulations of mesoscale convective systems over South America—A feature tracker intercomparison. *Journal of Geophysical Research: Atmospheres*, *129*(8), e2023JD040254. https://doi.org/10.1029/2023JD040254

Prill, F. (2020). *DWD ICON tools documentation* (Technical Report). Deutscher Wetterdienst (DWD).

Raschendorfer, M. (2001). The new turbulence parameterization of LM. *COSMO News Letter No. 1, Consortium for Small-Scale Modelling*, 89–97. Retrieved from http://www.cosmo-model.org

Rehbein, A., Ambrizzi, T., & Mechoso, C. R. (2018). Mesoscale convective systems over the Amazon basin. Part I: Climatological aspects. *International Journal of Climatology*, *38*(1), 215–229.

Reichle, R., Lannoy, G. D., D.Koster, R., Crow, W. T., Kimball, J. S., Liu, Q., & Bechtold, M. (2022). SMAP L4 global 3-hourly 9 km ease-grid surface and root zone soil moisture analysis update, version 7 [Dataset]. *NASA National Snow and Ice Data Center Distributed Active Archive Center*. https://doi.org/10.5067/LWJ6TF5SZRG3

Roca, R., & Fiolleau, T. (2020). Extreme precipitation in the tropics is closely associated with long-lived convective systems. *Communications Earth and Environment*, *1*(1), 18. https://doi.org/10.1038/s43247-020-00015-4

Schneider, L., Barthlott, C., Hoose, C., & Barrett, A. I. (2019). Relative impact of aerosol, soil moisture, and orography perturbations on deep convection. *Atmospheric Chemistry and Physics*, *19*(19), 12343–12359. https://doi.org/10.5194/acp-19-12343-2019

Schulz, J.-P., & Vogel, G. (2020). Improving the processes in the land surface scheme TERRA: Bare soil evaporation and skin temperature. *Atmosphere*, *11*(5), 513. https://doi.org/10.3390/atmos11050513

Silva, M. E. S., Pereira, G., & da Rocha, R. P. (2016). Local and remote climatic impacts due to land use degradation in the Amazon "Arc of Deforestation". *Theoretical and Applied Climatology*, *125*, 609–623. https://doi.org/10.1007/s00704-015-1516-9

Taylor, C. M. (2015). Detecting soil moisture impacts on convective initiation in Europe. *Geophysical Research Letters*, *42*(11), 4631–4638. https://doi.org/10.1002/2015GL064030

Taylor, C. M., Birch, C. E., Parker, D. J., Dixon, N., Guichard, F., Nikulin, G., & Lister, G. M. (2013). Modeling soil moisture-precipitation feedback in the Sahel: Importance of spatial scale versus convective parameterization. *Geophysical Research Letters*, *40*(23), 6213–6218. https://doi.org/10.1002/2013GL058511

Taylor, C. M., de Jeu, R. A., Guichard, F., Harris, P. P., & Dorigo, W. A. (2012). Afternoon rain more likely over drier soils. *Nature*, *489*(7416), 423–426. https://doi.org/10.1038/nature11377

Taylor, C. M., Gounou, A., Guichard, F., Harris, P. P., Ellis, R. J., Couvreux, F., & De Kauwe, M. (2011). Frequency of Sahelian storm initiation enhanced over mesoscale soil-moisture patterns. *Nature Geoscience*, *4*(7), 430–433. https://doi.org/10.1038/NGEO1173

Teramura, H., Sato, T., & Tamura, K. (2019). Observed evidence of enhanced probability of mesoscale convective system initiations due to land surface heterogeneity in semiarid East Asia. *SOLA*, *15*, 143–148. https://doi.org/10.2151/sola.2019-026

Wang, J., Chagnon, F. J., Williams, E. R., Betts, A. K., Renno, N. O., Machado, L. A., et al. (2009). Impact of deforestation in the Amazon basin on cloud climatology. *Proceedings of the National Academy of Sciences*, *106*(10), 3670–3674. https://doi.org/10.1073/pnas.0810156106

Web Services of Deutscher Wetterdienst. (2021). Web Services of Deutscher Wetterdienst. Retrieved from https://webservice.dwd.de/cgi-bin/spp1167/webservice.cgi

Werth, D., & Avissar, R. (2002). The local and global effects of Amazon deforestation. *Journal of Geophysical Research*, *107*(D20), 8087.

Williams, I. N. (2019). Evaluating soil moisture feedback on convective triggering: Roles of convective and land-model parameterizations. *Journal of Geophysical Research: Atmospheres*, *124*(1), 317–332. https://doi.org/10.1029/2018JD029326

Zängl, G., Reinert, D., Rípodas, P., & Baldauf, M. (2015). The ICON (ICOsahedral Non-hydrostatic) modelling framework of DWD and MPI-M: Description of the non-hydrostatic dynamical core. *Quarterly Journal of the Royal Meteorological Society*, *141*(687), 563–579. https://doi.org/10.1002/qj.2378